Journal of Alloys and Compounds 509 (2011) 6659–6665

Contents lists available at ScienceDirect

Journal of Alloys and Compounds

journal homepage: www.elsevier.com/locate/jallcom

# Sintering behaviors, magnetic and electric properties of Bi–Zn co-doped $Co_2Y$ ferrites

Hsing-I. Hsiang[a,*], Li-Then Mei[a], Chi-Shiung Hsi[b], Wei-Cheng Wu[c], Jer-Hao Wu[a], Fu-Su Yen[a]

[a] Department of Resources Engineering, Particulate Materials Research Center, National Cheng Kung University, 70101 Tainan, Taiwan, ROC
[b] Department of Materials Science and Engineering, National United University, Miaoli, Taiwan, ROC
[c] Inpaq Technology Co. Ltd., Miaoli, Taiwan, ROC

ARTICLE INFO

*Article history:*
Received 23 October 2010
Received in revised form 19 March 2011
Accepted 23 March 2011
Available online 1 April 2011

*Keywords:*
$Co_2Y$ ferrites
Sinting
Magnetic property
Electric property

ABSTRACT

The Bi and Zn substitution effects on the sintering behaviors, magnetic and electric properties of hexagonal ferrites with a composition of $2(Ba_{1-x}Bi_xO)\cdot2(Zn_yCo_{0.8-y}Cu_{0.2}O)\cdot6(Fe_{2-x/3}Zn_{x/3}O_3)$ were investigated. The results showed that the addition of Bi and Zn can significantly promote $Co_2Y$ densification. The Y phase may be triggered to decompose into M and spinel phases at high sintering temperatures (above 1050 °C) for samples with excess Bi ($x = 0.2$) substitution, which resulted in densification and magnetic properties degradation. $Co_2Y$ ferrites with $x = 0.1$ and $y = 0.4$ sintered at 1050 °C show a relative density of 94%, a high initial permeability of 4.5, a quality factor (Q) of 50.



## 1. Introduction

The most commonly used materials in inductors for high-frequency applications are NiCuZn ferrites [1], or non-magnetic materials such as low-temperature cofired ceramics [2]. The non-magnetic materials are used for high-frequency applications since NiCuZn ferrites (ferroxcube) typically exhibit severe property changes above 200 MHz due to the Snoek limit [3]. The frequency of maximum quality factor of chip inductors made of non-magnetic material is over 500 MHz. However, the quality factors at frequencies around 200–300 MHz are much lower than those at higher frequencies [4]. In addition, because chip inductors are prepared by winding a wire around a core of non-magnetic material, it is necessary to have a larger number of coil winding turns to obtain a desired inductance; thus limiting the miniaturization. Therefore, it is desirable to develop a magnetic material that has a higher quality factor than non-magnetic materials at 200–300 MHz, for use in making high frequency chip inductors. Magneto-plumbite ferrites with hexagonal structure have revealed a higher dispersion frequency than that of NiCuZn ferrites, which can be used in the high frequency applications [5–12]. Among those ferrites, the $Co_2Y$ ferrite $2(BaO)\cdot2(CoO)\cdot6(Fe_2O_3)$ have good magnetic properties (such as permeability and quality factor) above 200 MHz [13,14]. Zn substitution can promote the saturation magnetization ($M_s$), and hence increase the permeability of $Co_2Y$ ferrites [15]. The Cu for Co and Bi for Ba substitution can promote the densification of Y-type ferrites at low temperatures [16–18]. Pires Jŭnior and Costa et al. [19,20] investigated the dielectric and magnetic properties of $Co_2Y$ added with PbO and $Bi_2O_3$ and observed that the dielectric properties were strongly dependent on frequency and the addition of the additives, PbO and $Bi_2O_3$. However, to our best knowledge, there is no systematic study on the Bi–Zn co-doping effects on the sintering behaviors, electric and magnetic properties of $Co_2Y$ ferrites.

The objective of this study was to investigate the Bi and Zn substitution effects on the sintering behaviors, micro-structures, electric and magnetic properties of hexagonal ferrites with a composition of $2(Ba_{1-x}Bi_xO)\cdot2(Zn_yCo_{0.8-y}Cu_{0.2}O)\cdot6(Fe_{2-x/3}Zn_{x/3}O_3)$. The relationships between the chemical compositions, densification, micro-structures, electric and magnetic properties of $Co_2Y$ ferrites are presented.

## 2. Experimental procedures

Hexagonal ferrites with a composition of $2(Ba_{1-x}Bi_xO)\cdot2(Zn_yCo_{0.8-y}Cu_{0.2}O)\cdot6(Fe_{2-x/3}Zn_{x/3}O_3)$ were prepared from reagent-grade $BaCO_3$, $Bi_2O_3$, $SrCO_3$, $Co_3O_4$, CuO, ZnO and $Fe_2O_3$, mixed and then calcined at 1000 °C for 2 h. The calcined powders were ball-milled for 48 h using yttria tetragonal zirconia polycrystal (YTZ) balls. The BET specific surface area values of the ball-milled powders were about 7.5–10 $m^2/g$. The powders were dried at 120 °C in an electric oven with PVA added for granulation. The powders were dry-pressed at 110 MPa into toroidal bodies. These specimens were then debindered at 500 °C and sintered at 900–1050 °C for 2 h. The densities of the sintered samples were determined using the Archimedean method. The crystalline phase evolution was characterized using an X-ray diffractometer (XRD) with a Cu-Kα (Siemens, D5000). The microstructures of the sintered samples after thermal etching at 1000 °C

* Corresponding author. Tel.: +886 6 2757575x62821; fax: +886 6 2380421.
*E-mail address:* hsingi@mail.ncku.edu.tw (H.-I. Hsiang).

0925-8388/$ – see front matter © 2011 Elsevier B.V. All rights reserved.
doi:10.1016/j.jallcom.2011.03.133

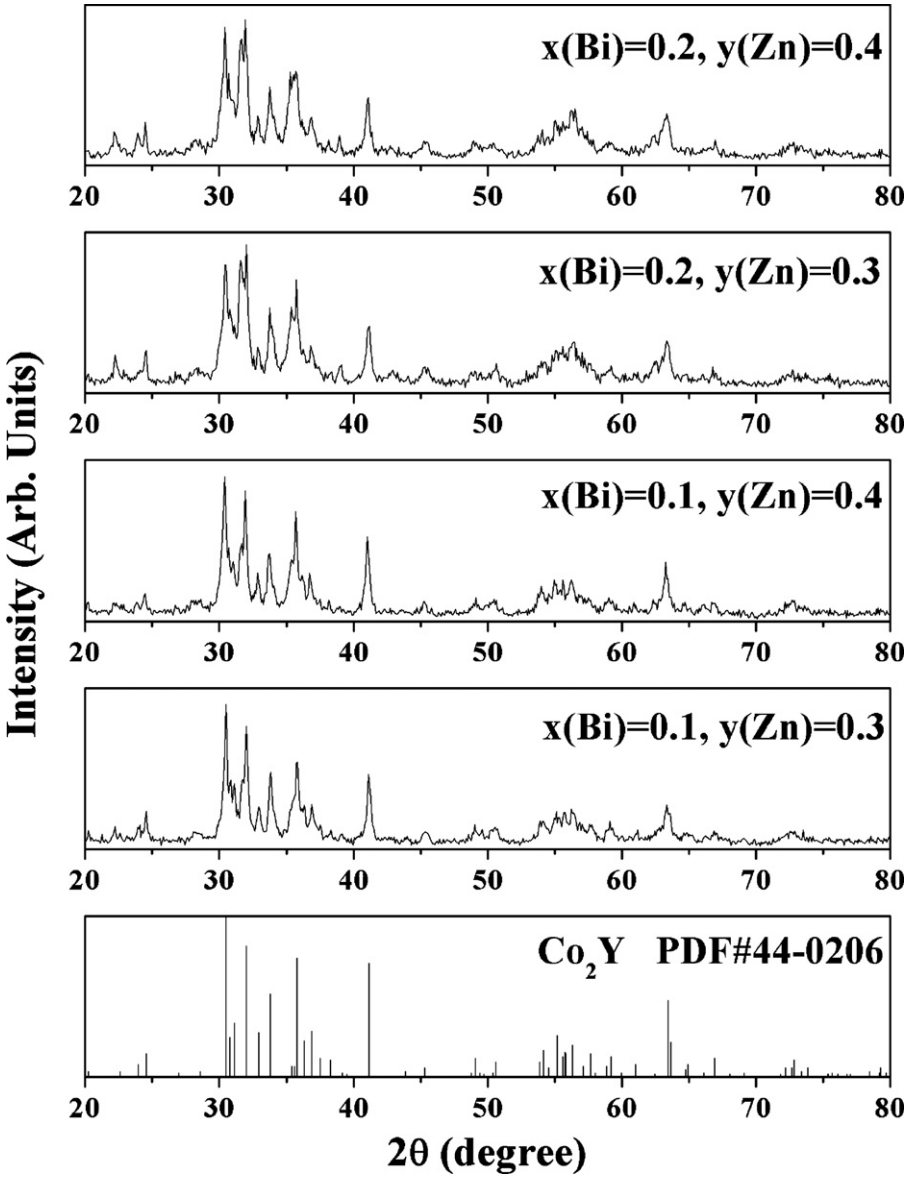


**Fig. 1.** XRD patterns of samples after calcination at 1000 °C.

for 30 min and then sputtering with Pt were examined using scanning electron microscopy (SEM) (Hitachi, S-4100). The impedance spectra from 20 Hz to 1 MHz were measured using HP 4284A. The initial permeability and dielectric constant were measured using an LCR meter (YHP 4291B, YHP Co., Ltd.) with HP 16454A magnetic material test fixture and HP 16453A dielectric material test fixture from 100 MHz to 1.8 GHz.

## 3. Results and discussion

Fig. 1 shows the XRD patterns of samples after calcination at 1000 °C. The XRD patterns for all samples exhibited a single $Co_2Y$ phase (ICDD PDF-Card 44-0206) with no second phase detected. Fig. 2 shows the XRD patterns of the samples after sintering at 1000 °C, indicating that only a single $Co_2Y$ phase was obtained with no second phase observed. However, as the sintering temperature was raised to 1050 °C, the $Co_2Y$ phase was accompanied by significant M and spinel phases as the main phases in the sample with $x = 0.2$ (Fig. 3), suggesting that the excess substitution of Bi for Ba may promote $Co_2Y$ ferrite decomposition into M and spinel phases at high sintering temperatures.

The relative densities of the samples with different $x$ and $y$ values as a function of the sintering temperature are shown in Fig. 4. For the samples with $x = 0.2$, the relative density increased and reached the maximum as the sintering temperature was raised from 900 °C to 1000 °C while the relative densities declined with further increasing the sintering temperature to 1050 °C. This may be due to the decomposition of $Co_2Y$ into M and spinel phases. The relative densities for the samples with $x = 0.1$ increased with sintering temperature. However, only the relative density of the sample with $y = 0.4$ sintered at 1050 °C could reach 93%. The other sintered sample with $x = 0.1$ did not result in comparable densification (relative density > 90%). These results suggest that the substitution of Bi for Ba can effectively promote $Co_2Y$ ferrite densification.

Fig. 5 shows SEM micrographs of the samples sintered at 1050 °C, indicating the grain size increased slightly with increasing Bi substitution ($x$ value) and the number of pores decreased with increasing Zn for Co substitution ($y$ value). Note that the sample with $x = 0.2$ has a larger and more well-formed hexagonal plate-like grain compared to the sample with $x = 0.1$, which may lead to a decrease in the relative density.

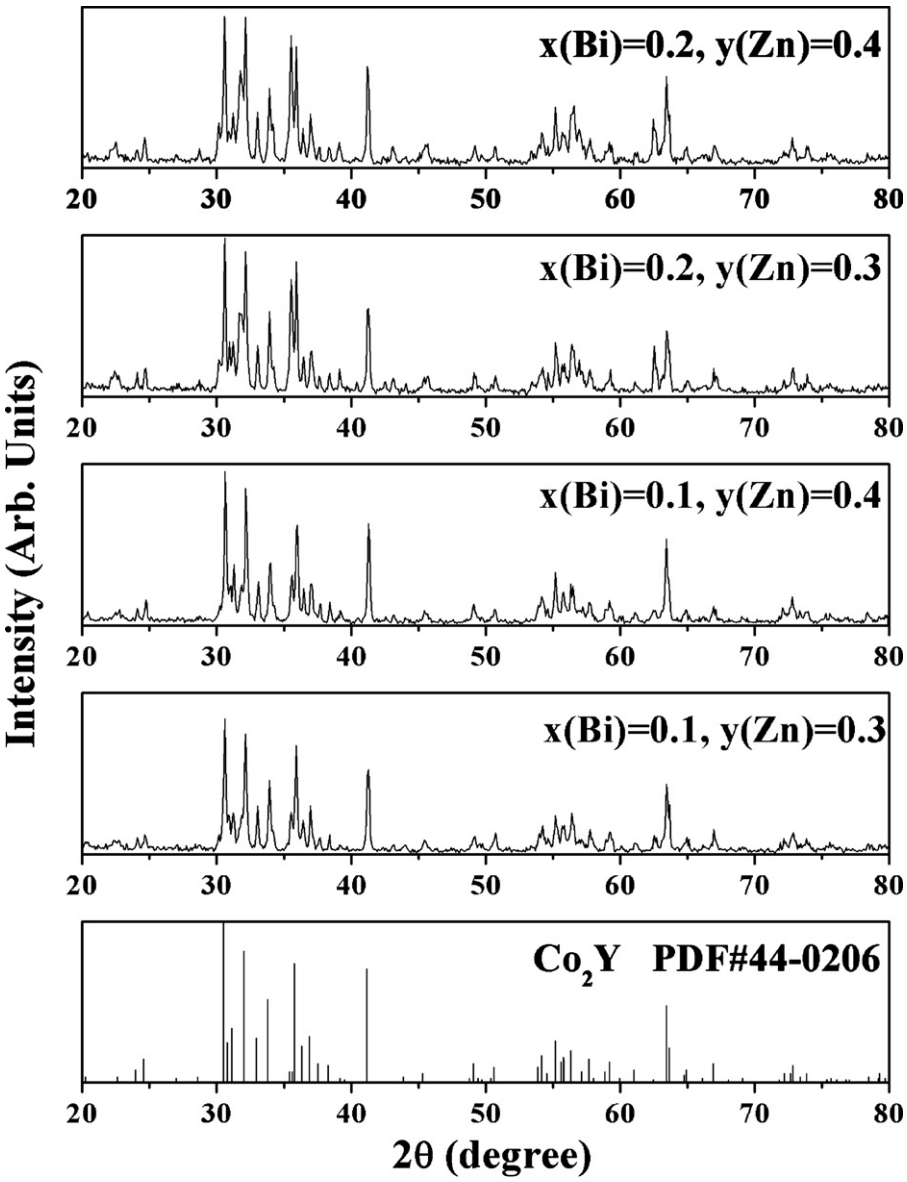


**Fig. 2.** XRD patterns of the samples after sintering at 1000 °C.

Fig. 6 shows the Cole–Cole plots for samples sintered at 1050 °C. The grain and grain boundary resistance determined from the Cole–Cole plots [21] are shown in Table 1. No great difference in the grain resistance was observed among the samples. The Zn for Co substitution made no difference in the grain boundary resistance. However, the grain boundary resistance decreased significantly as Bi substitution was increased from 0.1 to 0.2, which may result from $Co_2Y$ decomposition into M and spinel phases.

The variation in relative dielectric permittivity ($\varepsilon'$) with frequency for the samples sintered at 1000 °C and 1050 °C are shown in Figs. 7 and 8, respectively. The dependence of initial permeability on the frequency for the samples sintered at 1000 °C and 1050 °C are shown in Figs. 9 and 10. The summary of the relative dielectric permittivities and magnetic properties (initial permeabilities and quality factors) at 300 MHz for samples sintered at various temperatures are shown in Tables 2 and 3, respectively. All the samples showed pronounced dielectric humps near 1.5 GHz, which may be due to the ionic resonance [22]. For the samples with $x = 0.1$, the relative dielectric permittivity and initial permeability increased with increasing sintering temperature due to the increase in the relative density. The relative dielectric permittivities and initial permeabilities of the samples sintered below 1000 °C with $x = 0.2$ were both

**Table 1**
Grain and grain boundary resistance determined from the Cole–Cole plots.

| Composition | $R_{gb}$ | $R_g$ |
|---|---|---|
| $x = 0.1$, $y = 0.3$ | 40.35 MΩ | 1000 kΩ |
| $x = 0.1$, $y = 0.4$ | 39.03 MΩ | 948 kΩ |
| $x = 0.2$, $y = 0.3$ | 10.72 MΩ | 840 kΩ |
| $x = 0.2$, $y = 0.4$ | 8.79 MΩ | 830 kΩ |

**Table 2**
Summary of the relative dielectric permittivities at 300 MHz for samples sintered at various temperatures.

| Samples | Relative dielectric permittivity | | | |
|---|---|---|---|---|
| | 900 °C | 950 °C | 1000 °C | 1050 °C |
| $x = 0.1$, $y = 0.3$ | 13 | 14 | 17 | 20 |
| $x = 0.1$, $y = 0.4$ | 14 | 16 | 18 | 21 |
| $x = 0.2$, $y = 0.3$ | 15 | 14 | 20 | 10 |
| $x = 0.2$, $y = 0.4$ | 16 | 18 | 21 | 14 |

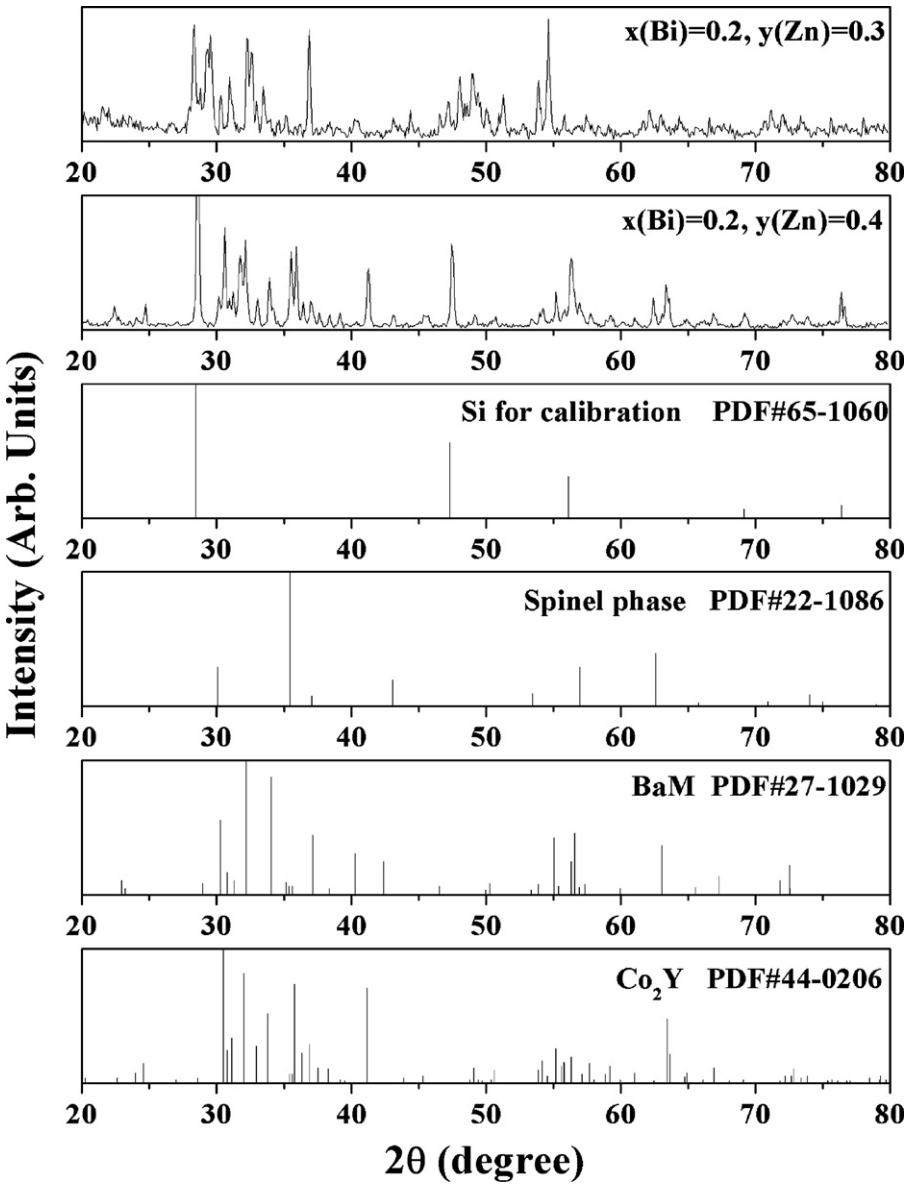


**Fig. 3.** XRD patterns of the samples after sintering at 1050 °C.

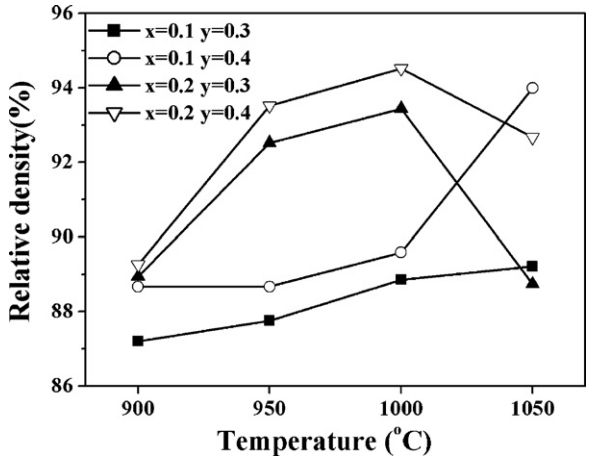


**Fig. 4.** Relative densities of the samples with different $x$ and $y$ values as a function of the sintering temperature.

higher than $x = 0.1$, because the Bi substitution for Ba promoted the densification of $Co_2Y$ ferrites. However, as the sintering temperature was raised from 1000 °C to 1050 °C, the relative dielectric permittivity decreased abruptly for the samples with $x = 0.2$. This may be caused by the decrease in relative density resulting from the decomposition of $Co_2Y$ into M and spinel phases. The permeability ($\mu$) of hexagonal polycrystalline ferrites can be expressed by [3]

$$\mu - 1 = \frac{8\pi M_s}{3H_a},$$

**Table 3**
Summary of the initial permeabilities ($\mu'$) and quality factors ($Q$) at 300 MHz for samples sintered at various temperatures.

| Sample | $\mu'/Q$ | | | |
|---|---|---|---|---|
| | 900 °C | 950 °C | 1000 °C | 1050 °C |
| $x = 0.1$, $y = 0.3$ | 2.9/20 | 2.9/20 | 3.5/10 | 4.4/30 |
| $x = 0.1$, $y = 0.4$ | 3.0/40 | 3.2/30 | 3.7/30 | 4.5/50 |
| $x = 0.2$, $y = 0.3$ | 3.2/40 | 2.9/40 | 3.9/40 | 3.8/10 |
| $x = 0.2$, $y = 0.4$ | 3.2/80 | 3.4/90 | 4.2/70 | 4.0/30 |

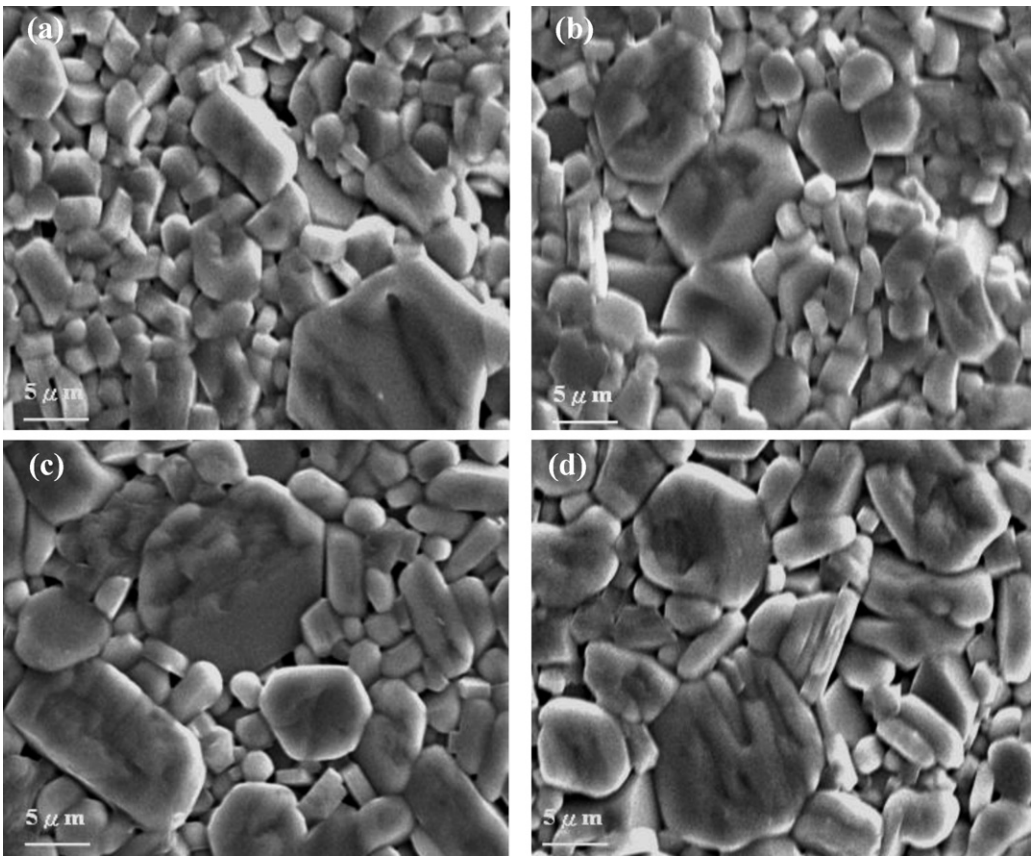


**Fig. 5.** SEM micrographs of the samples sintered at 1050 °C (a) $x = 0.1$, $y = 0.3$; (b) $x = 0.1$, $y = 0.4$; (c) $x = 0.2$, $y = 0.3$ and (d) $x = 0.2$, $y = 0.4$.

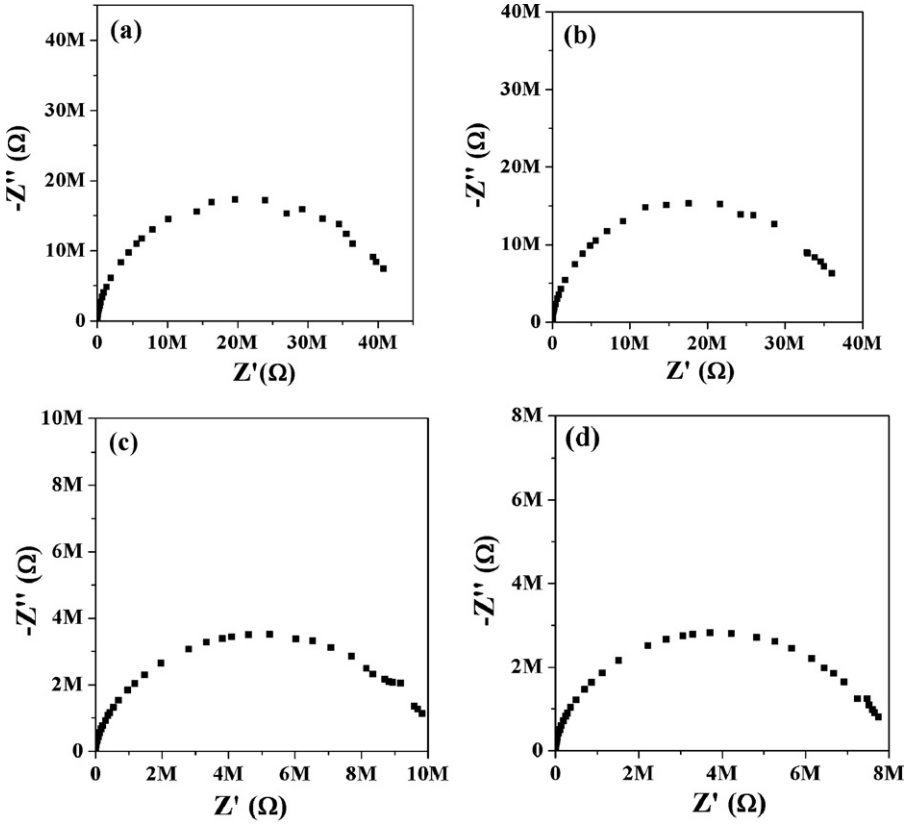


**Fig. 6.** Cole–Cole plots for samples sintered at 1050 °C (a) $x = 0.1$, $y = 0.3$; (b) $x = 0.1$, $y = 0.4$; (c) $x = 0.2$, $y = 0.3$ and (d) $x = 0.2$, $y = 0.4$.

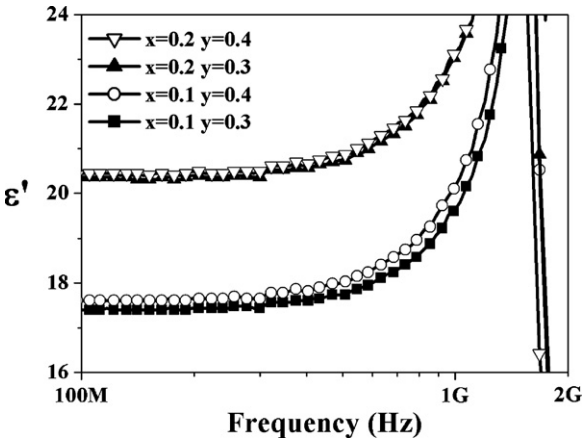


**Fig. 7.** Variation in relative dielectric permittivity ($\varepsilon'$) with frequency for the samples sintered at 1000 °C.

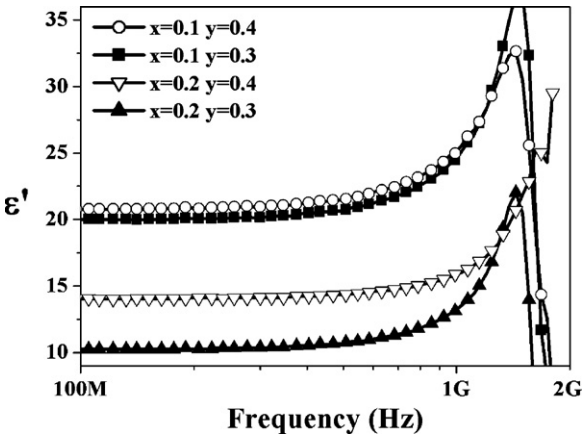


**Fig. 8.** Variation in relative dielectric permittivity ($\varepsilon'$) with frequency for the samples sintered at 1050 °C.

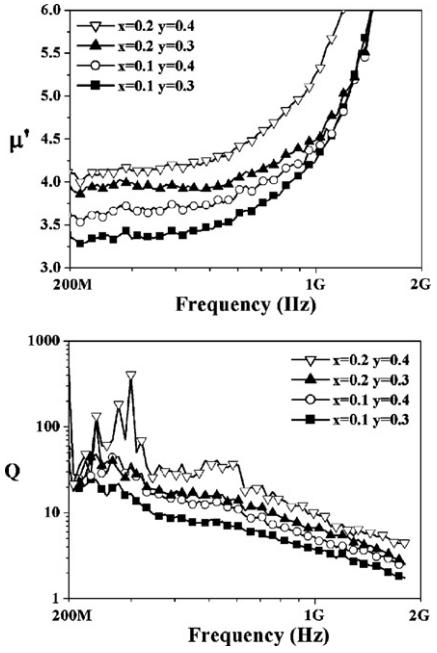


**Fig. 9.** Dependence of initial permeability and quality factor ($Q$) on the frequency for the samples sintered at 1000 °C.

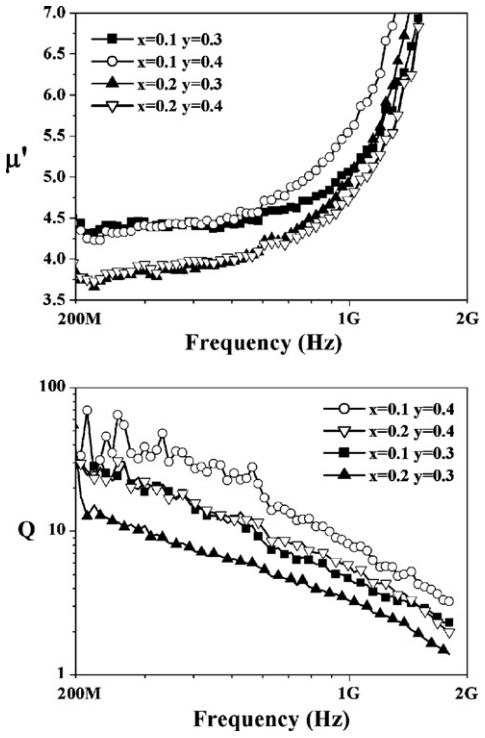


**Fig. 10.** Dependence of initial permeability and quality factor ($Q$) on the frequency for the samples sintered at 1050 °C.

where $M_s$ is the saturation magnetization and $H_a$ is the anisotropic field. Zn substitution for Co will promote the permeability through increasing $M_s$ and decreasing $H_a$. Therefore, the initial permeabilities of the samples with $y = 0.4$ were all higher than $y = 0.3$. The substitution of excess Bi ($x = 0.2$) may degrade the permeability due to the promotion of Y phase decomposition into M phase and the decrease in the relative density. The dependence of the $Q$ value on the sintering temperature and the chemical composition (Figs. 9 and 10) has the same trend with Fig. 4. For the sample with $x = 0.1$, the $Q$ value increased with increasing sintering temperature, which may result from the increase of the relative density. However, the $Q$ value decreased with increasing sintering temperature due to the decrease of density for the sample with $x = 0.2$. These results suggest that the $Q$ value mainly depends on the relative density. Note that $Co_2Y$ ferrites with $x = 0.1$ and $y = 0.4$ sintered at 1050 °C show a relative density of 94%, a high initial permeability of 4.5, a quality factor ($Q$) of 50 and the resonance frequency above 500 MHz, which can be used in inductors for high frequency applications.

## 4. Conclusions

(1) The densification of $Co_2Y$ can be significantly promoted by the substitution of Bi and Zn.
(2) The initial permeability of $Co_2Y$ can be improved by the Zn substitution for Co.
(3) The substitution of excess Bi ($x = 0.2$) may degrade the initial permeability and relative dielectric permeability due to the promotion of Y phase decomposition into M phase and the decrease in the relative density.
(4) The $Co_2Y$ ferrites with $x = 0.1$ and $y = 0.4$ sintered at 1050 °C show a relative density of 94%, a high initial permeability of 4.5, a quality factor ($Q$) of 50 and the resonance frequency above 500 MHz, which can be used in inductors for high frequency applications.

## Acknowledgments

This work was financially sponsored by the National Science Council of the Republic of China and Inpaq technology Co. Ltd. (NSC 98-2622-E-006-011-CC2).

## References

[1] T. Nakamura, J. Magn. Magn. Mater. 168 (1997) 285–291.
[2] J.Y. Hsu, H.C. Lin, H.D. Shen, IEEE Trans. Magn. 33 (1997) 3325–3327.
[3] J. Smith, H.P.J. Wijn, Ferrites, Philips Technical Library, Eindhoven, Netherlands, 1959.
[4] G.J. Jonker, H.P.J. Wijn, P.B. Braun, Philips Tech. Rev. 18 (1956) 145.
[5] H.I. Hsiang, L.T. Mei, C.S. Hsi, W.C. Wu, L.B. Cheng, F.S. Yen, J. Alloys Compd. 509 (2011) 3343–3346.
[6] H.I. Hsiang, R.Q. Yao, Mater. Chem. Phys. 104 (2007) 1–4.
[7] H.I. Hsiang, L.T. Mei, C.S. Hsi, W.C. Wu, L.B. Cheng, F.S. Yen, J. Magn. Magn. Mater. 323 (2011) 1011–1014.
[8] H.I. Hsiang, Jpn. J. Appl. Phys. 41 (2002) 5137–5141.
[9] J. Xu, G. Ji, H. Zou, Y. Zhou, S. Gan, J. Alloys Compd. 509 (2011) 4290–4294.
[10] L. Jia, J. Luo, H. Zhang, G. Xue, Y. Jing, J. Alloys Compd. 489 (2010) 162–166.
[11] J. Xu, H. Zou, H. Li, G. Li, S. Gan, G. Hong, J. Alloys Compd. 490 (2010) 552–556.
[12] N. Chen, K. Yang, M. Gu, J. Alloys Compd. 490 (2010) 609–612.
[13] J.L. Snoek, Physica 14 (1948) 207–217.
[14] X.C. Li, R.Z. Gong, Z. Feng, J. Yan, X. Shen, H. He, J. Am. Ceram. 89 (2006) 1450–1452.
[15] Y. Bai, J. Zhou, Z. Gui, L. Li, L. Qiao, J. Alloys Compd. 450 (2008) 412–416.
[16] Y. Bai, J. Zhou, Z. Gui, L. Li, J. Magn. Magn. Mater. 278 (2004) 208–213.
[17] Y. Bai, J. Zhou, Z. Gui, Z. Yue, L. Li, Mater. Sci. Eng. B99 (2003) 266–269.
[18] X.C. Li, R.Z. Gong, Z. Feng, J.B. Yan, X. Shen, H.H. He, J. Am. Ceram. Soc. 89 (2006) 1450–1452.
[19] G.F.M. Pires Júnior, H.O. Rodrigues, J.S. Almeida, E.O. Sancho, J.C. Góes, M.M. Costa, J.C. Denardin, A.S.B. Sombra, J. Alloys Compd. 493 (2010) 326–334.
[20] M.M. Costa, G.F.M. Pires Júnior, A.S.B. Sombrab, Mater. Chem. Phys. 123 (2010) 35–39.
[21] J.R. Macdonald, W.B. Johnson, in: E. Barsoukov, J.R. Macdonald (Eds.), Impedance Spectroscopy Theory, Experiment, and Applications, A John Wiley & Sons, Inc., Hoboken, NJ, 2005, pp. 1–26.
[22] W.D. Kingery, H.K. Bowen, D.R. Uhlmann, Introduction to Ceramics, 2nd ed., 1976, p. 922.